
Article:
Ogirigbo, OR and Black, L orcid.org/0000-0001-8531-4989 (2016) Influence of slag composition and temperature on the hydration and microstructure of slag blended cements. Construction and Building Materials, 126. pp. 496-507. ISSN 0950-0618

https://doi.org/10.1016/j.conbuildmat.2016.09.057

Influence of slag composition and temperature on the hydration and microstructure of slag blended cements

Okiemute Roland Ogirigbo[a], Leon Black[b,*]

[a,b]Institute of Resilient Infrastructure, School of Civil Engineering, University of Leeds, Woodhouse Lane, Leeds LS2 9JT, United Kingdom

[a]cnoro@leeds.ac.uk, [b]L.Black@leeds.ac.uk

*Corresponding author. Tel: +44113 343 2283, Email address: L.Black@leeds.ac.uk

ABSTRACT

GGBS is used extensively as a cement replacement material, reducing the carbon footprint of cement while potentially improving technical performance. However, standards consider hydration of slag composite cements only at 20°C. This may not be applicable for use in tropical climates. This work has investigated the impact of GGBS composition and curing temperature on the hydration, microstructure and subsequent transport properties of such composite cements. Two slags, of differing compositions, were combined with a CEM I 52.5 R at 30% replacement. Paste samples were characterised by calorimetry, TGA, XRD and SEM to follow hydration and microstructural development. Mortar samples were used to follow strength development and water transport properties. All tests were carried out at temperatures of 20 and 38°C. The higher temperature resulted in an increase in the degree of hydration of the slags, but had a deleterious impact on the microstructure. The more basic slag had higher strengths and greater degrees of hydration especially at the high temperature. The results showed that temperature had a much greater influence on the reactivity of the slags than the difference in chemical composition.

Keywords: GGBS, slag composition, temperature, hydration, microstructure, slag blends

1. Introduction

GGBS is a by-product from iron manufacture. The molten iron slag from the blast furnace is quenched with water or steam to produce a glassy and granular material, which is grounded to a fine powder to produce GGBS. The material has almost the same fineness and specific surface area as Portland cement [1]. The material is glassy in nature and latently hydraulic [2], and its use in mortar and concrete has been specified by various standards [3, 4]. However, the nature of the ore, composition of the limestone flux, coke consumption and the type of iron being made are factors which affect the chemical composition of GGBS [5].

The hydraulicity of GGBS depends mainly on its chemical composition, glass content, particle fineness, alkalinity of the reacting system and temperature at the early stages of hydration [6]. The hydraulicity increases with the particle fineness [7] and the glass content. Typical glass content of GGBS vary between 85 and 90% [8]. BS EN 197-1:2011 [9] specifies that at least two-third of the mass of the slag must be glassy, although research data show that slag samples with as little as 30–65% glass contents are still suitable [10].

The oxides of calcium, magnesium and aluminium are known to increase the hydraulicity of GGBS, while those of silicon and manganese decrease it [11]. MgO has the same influence as CaO up to about 11% by weight [5]. Increasing the Al_2O_3 content to 13% and above will result in an increase in early strength and a decrease in the later strength [12]. Wang et al. [13] observed a positive correlation between the Al_2O_3 content and the reactivity of the slags, for slags having a CaO content greater than 37%. In another study by Ben Haha et al. [11, 14], it was observed that the reactivity of the slags increased with the magnesia content. As they increased the alumina content, the reactivity of the slags was reduced at early ages, but became similar at

later ages beyond 28 days. However, of the three slags they studied, the CaO content of the two high alumina slag was less than 37%. For other oxides like P_2O_5, the influence depends on the clinker type and test age, but generally has a positive influence beyond 28 days of curing. Oxides of tin and iron, as well as sulphur, seem not to have any effect [5].

Ratios of these oxides have been used by various standards to assess the hydraulicity of a slag. For example, EN 197-1:2011 prescribes that for GGBS, the (CaO + MgO)/SiO_2 ratio by mass must exceed 1 [9]. Several workers [5, 10, 15], have also suggested other oxide ratios, some of which have been shown in Table 4. However, previous studies [10, 15-17] have shown that these ratios do not necessarily give accurate prediction of a slag's performance. More so, it becomes more complex when other factors like changes in temperature are considered.

The contribution of GGBS to the heat of hydration increases with temperature, due to the accelerating effect of temperature on slag reactivity [18-21], and as a result has been reported to be very beneficial for use in hot weather concreting [5]. For example, Wu et al. [20] studied the influence of temperature on the early stage hydration of PC slag blends using isothermal calorimetry and chemical shrinkage. They used three different PC slag blends comprising of 40, 50 and 65% of slag. All three blends were hydrated at temperatures of 15, 27, 38 and 60℃. They observed th at the slag reacted more slowly than the PC component at 15℃ and at an accelerated rat e at temperatures above 27℃. Substantial portions of the slag had reacted within the firs t 24 hours at temperatures of 27℃ and above. Similar findings were also re ported by others [22-27].

In all these studies, the issue of how changes in temperature affect the hydration process of slags of different chemical compositions was not fully explored. This will be

of importance due to the widespread use of GGBS as a cementitious material in tropical climatic regions. This paper looks at how variation in chemical composition of slag coupled with a change in temperature will affect the hydration process of slag blended cements, and how this relates to the microstructure and subsequent transport properties.

2. Experimental programme

2.1 Materials

Two slags were combined with a CEM I 52.5 R at 30% replacement level to produce slag blends designated as S1 and S2 respectively. Both slags had similar physical properties, with different chemical compositions (notably the alumina and silica contents). The oxide and phase composition of the as-received slags and cement are shown in Table 1 and Table 2 respectively. The X-ray diffraction showing the amorphous and crystalline phases and the particle size distribution of the slags are shown in Fig. 1 and Fig. 2 respectively. Other physical properties of the cementitious materials are shown in

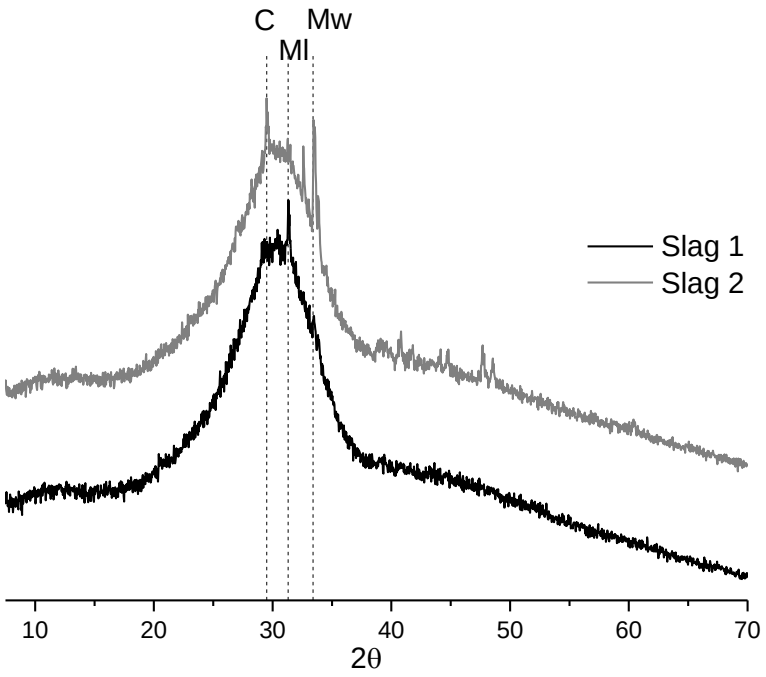

C - Calcite, Ml - Melilite, Mw - Merwinite

Fig. 1: XRD of the as-received slags

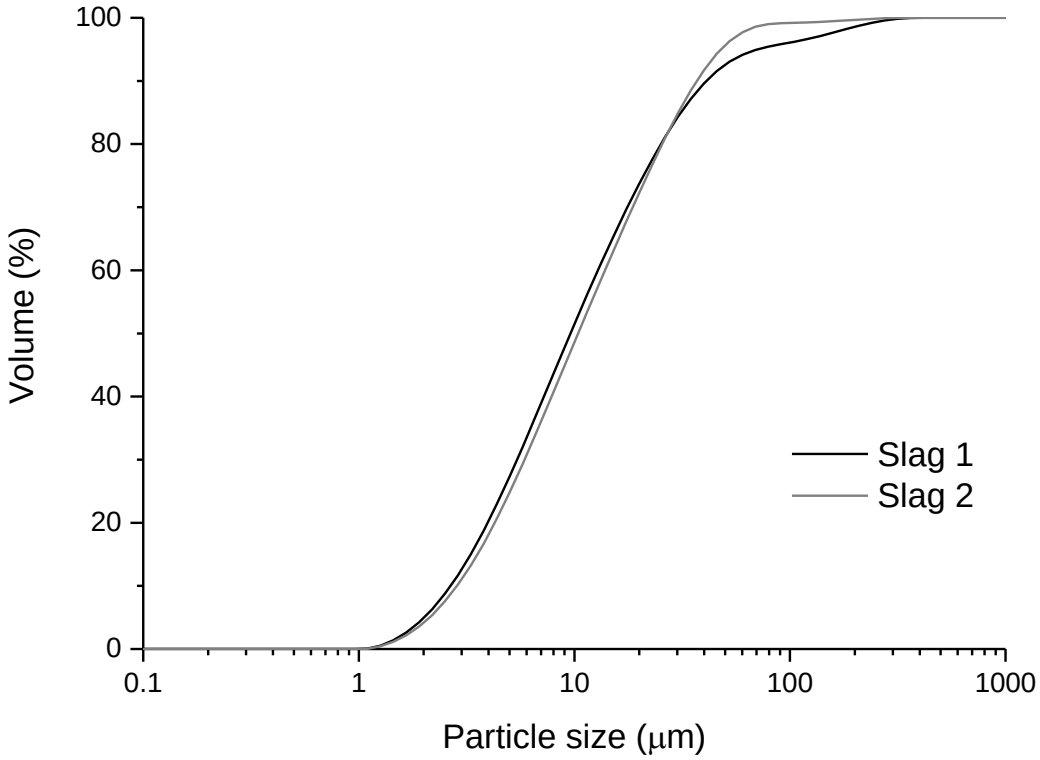

Fig. 2: Particle size distribution of the slags

Table 3.

96

97 **Table 1:** Oxide composition of the starting materials

Property	Unit	CEM I 52.5 R	Slag 1	Slag 2
LOI at 950℃	%	2.54	(+1.66)*	(+0.40)*
SiO_2	%	19.10	36.58	40.14
Al_2O_3	%	5.35	12.23	7.77
TiO_2	%	0.25	0.83	0.30
MnO	%	0.03	0.64	0.64
Fe_2O_3	%	2.95	0.48	0.78
CaO	%	62.38	38.24	37.9
MgO	%	2.37	8.55	9.51
K_2O	%	1.05	0.65	0.55
Na_2O	%	0.05	0.27	0.36
SO_3	%	3.34	1.00	1.47
P_2O_5	%	0.10	0.06	0.02
Sum at 950℃	%	99.50	99.88	99.43

98 *The sample was oxidized with HNO_3 before the determination of LOI

Table 2: Crystalline phases of the cementitious materials

Phase	Unit	CEM I 52.5R	Slag 1	Slag 2
Alite, C_3S	%	62.1		
Belite, C_2S	%	8.9		
Aluminate, C_3A	%	9.1		
Ferrite, C_4AF	%	8.5		
Calcite	%	1.8	0.3	0.5
Anhydrite, AH	%	0.6		
Hemihydrate, HH	%	2.4		
Gypsum	%	1.7		
Merwinite	%		<0.1	2.3
Akermanite	%		0.2	<0.1
Illite	%		0.2	<0.1
Gehlenite	%		<0.1	<0.1
Glass content	%		99.3	97.1
Others	%	5.0		
Total	%	100.1	100	100

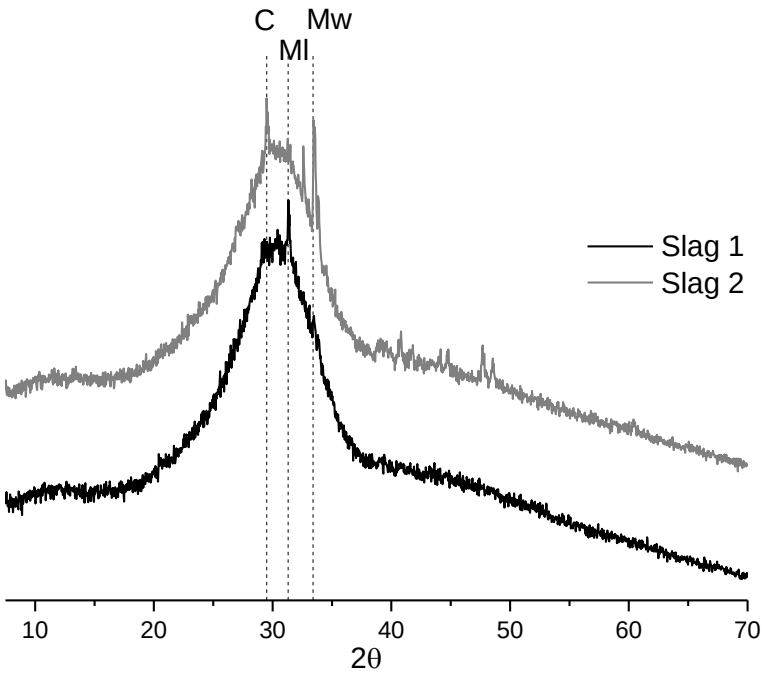

C - Calcite, Ml - Melilite, Mw - Merwinite

Fig. 1: XRD of the as-received slags

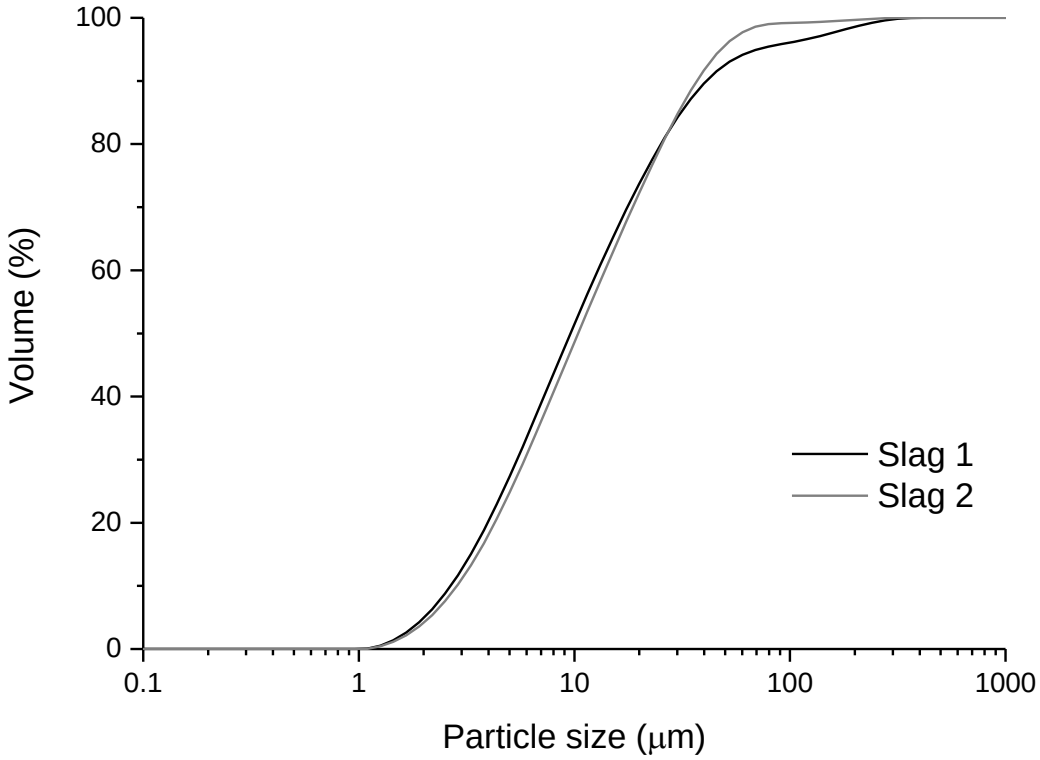

Fig. 2: Particle size distribution of the slags

Table 3: Physical properties of cementitious materials

Property	Unit	CEM I 52.5 R	Slag 1	Slag 2
Density	g/cm^3	3.18	2.94	2.95
Blaine	m^2/kg	571	449	409
Particle size, d50	µm	-	11.0	11.9

2.2 Reactivity of the slags

The basicity and activity indices shown in Table 4 have been used for the initial classification of the slags. The basicity index gives an indication of the slag's hydraulicity while the activity index shows how the slag will contribute to strength development. The activity index is defined as the ratio (in percent) of the compressive strength of the combination (by mass) of 50% of the slag with 50% of the test cement, to the compressive strength of the test cement on its own [3]. A CEM I 52.5 R was used as the test cement.

Table 4: Basicity and activity indices of the slags

Basicity/ hydraulic index			
	Requirement for good performance	Slag 1	Slag 2
CaO/SiO_2	1.3 – 1.4 [10]	1.05	0.94
$(CaO + MgO)/SiO_2$	> 1.0 [9]	1.28	1.18
$(CaO + MgO + Al_2O_3)/ SiO_2$	≥ 1.0 [28]	1.61	1.37
Activity index (%)			
7 day	> 45% [3]	58.8	53.6
28 day	> 70% [3]	84.3	84.3

2.3 Details of mixes and curing conditions

The composite cements were prepared by blending the slags and the CEM I 52.5 R in a laboratory ball mill using plastic charges. Two blends were used for this study, each containing 30% slag and 70% CEM I 52.5 R, and designated S1 and S2 for slag 1 and slag 2 respectively. A water/binder ratio (w/b) of 0.5 was used for all mixes. Mortar samples were prepared from the blends in accordance to EN196-1:2005 [29]. Mortar prisms of 40 x 40 x 160 mm were used for compressive strength tests, while 50 mm mortar cubes were used for sorptivity tests. Cement paste samples were also prepared from the blends using the same w/b ratio of 0.5. These were used for the isothermal calorimetry, thermal analysis, and XRD and SEM studies.

2.3.1 Curing at 20 and 38℃:

For samples cured at 20℃, mixing and casting was done under normal laboratory conditions (temperature of 20 ± 2℃), with samples remaining in their moulds for one day, after which they were demoulded and cured under water at 20℃.

For samples cured at 38℃, the starting materials and moulds were preconditioned in an oven at 38℃ overnight. Mixing and casting was done at normal laboratory conditions. After casting, the moulds were covered with thin polythene sheets and immediately transferred to a pre-heated oven at 38℃. Samples were demoulded after 1 day and subsequently cured under water in water baths maintained at 38℃.

2.4 Test methods

2.4.1 Isothermal calorimetry

The heat flow generated during hydration was measured for cement pastes using a TAM Air 8 twin channel calorimeter. Measurements were obtained on 9 grams of cement paste for a period of 28 days at 20 and 38℃. Calorimetry was used qualitatively to measure the degree of reaction of the slag. This was done by replacing

140 the slag component in the slag blends with quartz of similar fineness as the slags [30-
141 32], to determine the filler effect. This enabled the heat contribution from the slag
142 during hydration to be separated from that of the cement. The difference between the
143 quartz- and slag blends can be ascribed to hydration of the slag.

144 2.4.2 BSE-SEM image analysis

145 2 mm thick discs cut from the central portions of 14 mm ϕ cylindrical hydrated cement
146 paste samples were hydration stopped by solvent exchange in isopropanol. Samples
147 were then resin impregnated and polished before BSE-SEM imaging using a Carl
148 Zeiss EVO SEM. An accelerating voltage of 15 keV was used, combined with a spot
149 size of 500. A total of 50 electron images were collected per sample at a magnification
150 of x800 and a working distance of 8 – 8.5 mm, and were analysed to determine the
151 degree of hydration. Magnesium elemental maps were used to distinguish between
152 anhydrous slag and portlandite (which have a similar grey level in a BSE image) [30,
153 32-34].

154 The degree of hydration was determined for 7 and 28 day old samples using the
155 expression below [30, 34]:

$$DR_{SEM}^{SCM}(t) = 1 - \frac{V_{(t)SCM}}{V_{(0)SCM}} \quad (1)$$

156 where:

157 $V_{(0)SCM}$ volume fraction of unreacted SCM before hydration,

158 $V_{(t)cem}$ volume fraction of unhydrated cement at hydration time t, and

159 $V_{(t)SCM}$ volume fraction of unreacted SCM at hydration time t.

160 Image analysis was also carried out on the electron images to determine the coarse
161 porosity. The approach used was similar to that used previously [35-37]. The degree

of capillary porosity was determined for 7 and 28 day old samples, cured at temperatures of 20 and 38℃.

2.4.3 Unconfined compressive strength

Compressive strength was determined in accordance with the procedure outlined in EN196-1:2005 [29] for mortar samples. Compressive strength was determined at 1, 7, 28, 90 and 180 days. At the test date, the samples were brought out from the curing tubs and split into two halves to produce six 40 x 40 x 80 mm samples, which were used for the test. The test was performed on a Tonipact 3000 concrete cube crusher.

2.4.4 Thermal analysis

Simultaneous thermal analysis (STA) was carried out using a Stanton Redcroft 780 series. About 15 to 18 mg of cement paste samples, whose hydration had been stopped by solvent exchange with isopropanol, were weighed and placed in an empty platinum crucible. A corresponding empty platinum crucible was used as the reference. Both the sample and the reference were heated under a nitrogen atmosphere from 20 to 1000℃ at a constant rate of 10℃/min. The portl andite (CH) content was determined using the tangent method [33] and was calculated using Equation 2. The bound water content (W_n) was taken as the difference between the mass loss at 50 and 550℃, at which point it was assumed that all the pha ses containing water had fully decomposed [32]. W_n, normalized to the total mass loss at 550℃ was calculated using Equation 3.

$$\%CH = CH_w \times \left(\frac{M_{CH}}{M_{H2O}}\right) \quad (2)$$

$$W_n = \left(\frac{W_{50} - W_{550}}{W_{550}}\right) \times 100 \quad (3)$$

where:

CH_w mass loss of water bound to CH

184 M_{CH} molar mass of CH, taken as 74g/mol

185 M_{H2O} molar mass of water, taken as 18g/mol

186 W_{550} mass loss at 550℃

187 W_{50} mass loss at 50℃

188 2.4.5 Sorptivity

189 Sorptivity was determined using similar methods as used by Tasdemir [38], and
190 Güneyesi [39]. Triplicate 50 mm mortar samples were used for the test. The samples
191 were cured for 28 and 90 days at 20 and 38℃, after which they wer e dried to constant
192 mass in an oven at 50℃. This process took 20 to 35 days depending on the mix and
193 age of the sample. After drying, the sides of the samples were coated with paraffin
194 and weighed to obtain the initial mass before they were placed in a 5mm deep trough
195 of water at 20℃. The sample mass es were recorded at predetermined times (1, 4, 9,
196 16, 25, 36, 49 and 64 mins). At each of these times, the mass of water absorbed by
197 each specimen was calculated by subtracting the initial mass from the recorded mass,
198 and from this the sorptivity coefficient (k) can be determined using the following
199 expression:

$$k = \frac{Q}{A\sqrt{t}} \quad (4)$$

200 where:

201 Q amount of water absorbed in m^3, which was calculated by dividing the
202 mass of the water absorbed in kg, by the density of water (1000 kg/m^3)

203 t time in seconds

204 A cross-sectional area of the specimen that was in contact with the water
205 in m^2

206 k sorptivity coefficient in $m^3/m^2s^{1/2}$.

3. Results and discussion

3.1 Unconfined compressive strength (UCS)

Fig. 3 shows the development of UCS at 20 and 38℃. Curing at elevated temperature led to increased strength up to 7 days, but with minimal strength gain beyond 28 days. Ultimately, the strengths of the samples cured at 20℃ were greater than those cured at 38℃. This is consistent with previous findings [24, 25, 27] and can be attributed to the effect of high temperature curing, which would result in a high initial rate of hydration and slower subsequent hydration rates [24, 40].

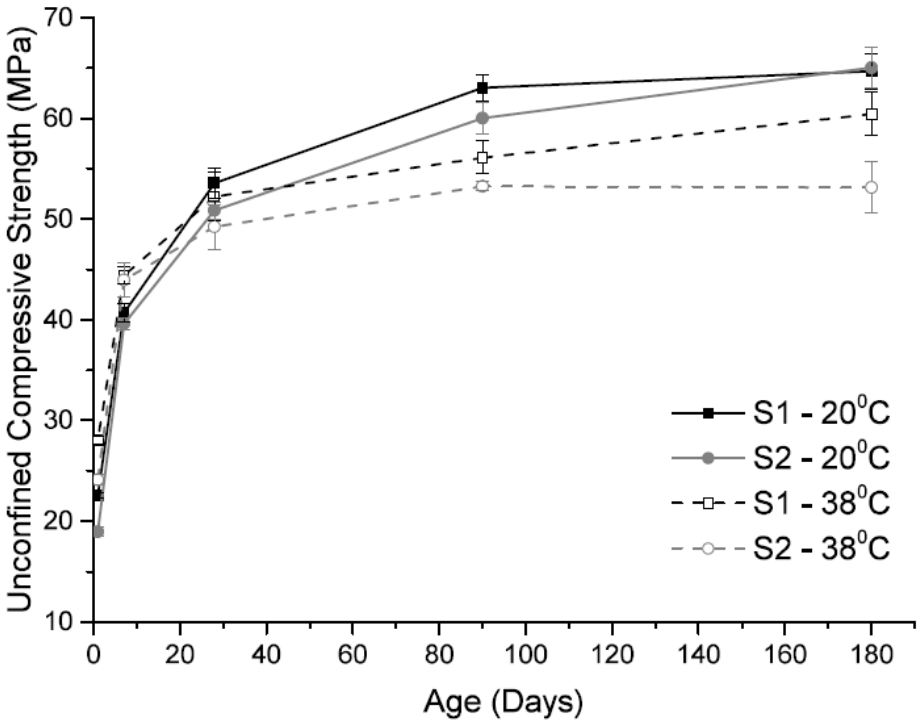

Fig. 3: Compressive strength for mixes made from slag 1 and slag 2 at 20 and 38℃

At 20℃ there was no significant difference in the UCS of the two slag blends, especially at later ages, whereas at 38℃, there was a clear distinction; with slag 1, the more basic slag, performing better than slag 2 at all ages. This implies that at the early ages, the difference in chemical composition of the slags had a greater influence on the strength performance; whereas at the later ages beyond 90 days, curing temperature had a greater influence on the strength performance of the slag blends.

As was shown in Table 4, variously proposed basicity indices would predict higher strengths for the more basic slag. However, this was not so, especially at the lower temperature of 20℃. This reinforces previous findings that basicity indices are not always a good predictor of performance [15, 16, 41]. On the other hand, in agreement with the study by Otieno et al [42], the strength performance at 20℃ was seen to tall y with the prediction of the activity index, which indicated that slag 1 would have better early age strength performance than slag 2, but similar later age strength performance. However, at the higher temperature of 38℃, the prediction of the basicity ind ices was seen to tally with the strength performance of the slag blends.

3.2 Degree of hydration of the slags

3.2.1 Heat of hydration from isothermal calorimetry

The calorimetry results obtained for the paste samples are shown in **Error! Reference source not found.** and **Error! Reference source not found.**. **Error! Reference source not found.**a and **Error! Reference source not found.**b show the heat flow measured for the slag blends over the first 60 hrs of reaction at 20 and 38℃ respectively, while **Error! Reference source not found.**c and **Error! Reference source not found.**d show the total heat evolved by the slag blends at 20 and 38℃ respectively, for a period up to 30 days (720 hrs). **Error! Reference source not found.**a and **Error! Reference source not found.**b show the positive contribution of the slag hydration to the total heat evolution at 20 and 38℃ respectively.

The addition of either quartz or slag to the CEM I resulted in a slight acceleration of the alite hydration, as can be observed from **Error! Reference source not found.**a and **Error! Reference source not found.**b, where the principal exotherm for S1, S2 and PC-30Q appeared slightly earlier than that for the CEM I. This can be attributed to the filler effect [31, 33, 43, 44], where during the early stages of the reaction, the

lack of reaction of either the quartz or slag allow more space for clinker hydrates to form [33, 44].

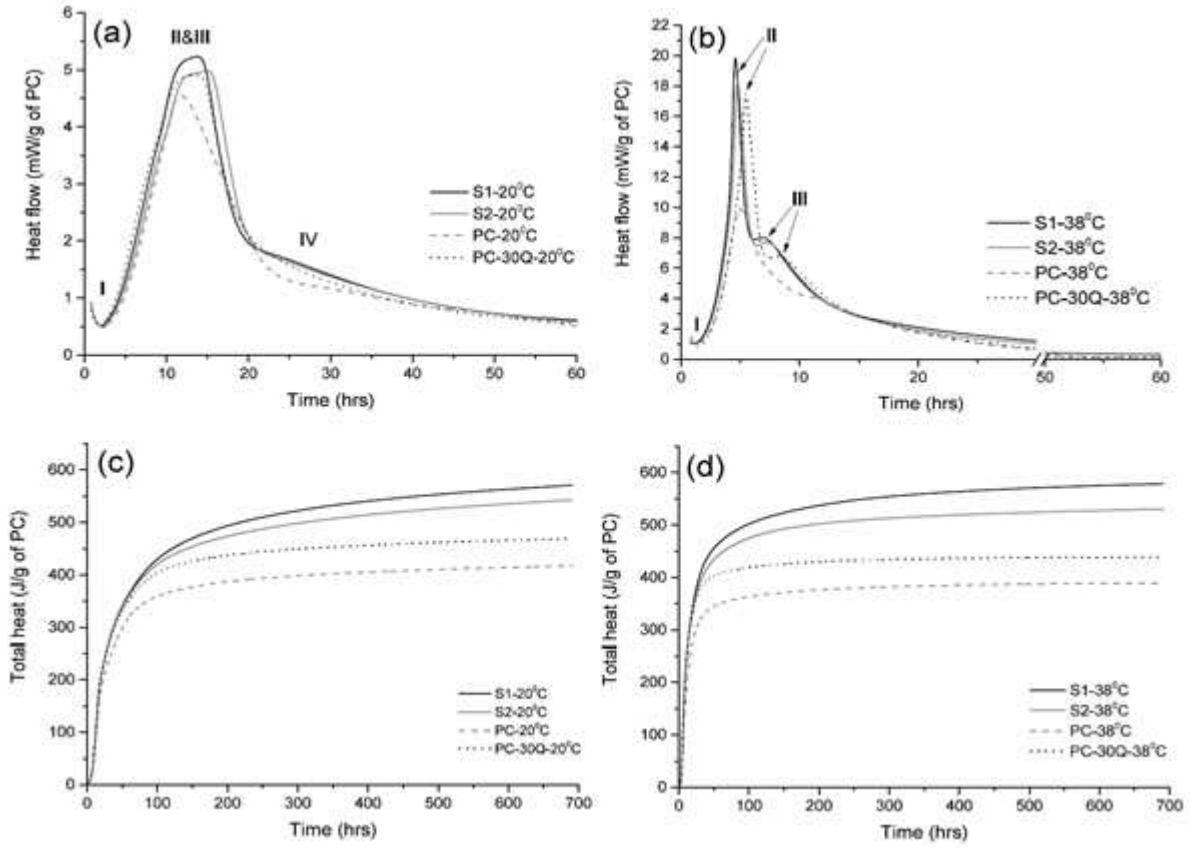

Fig. 4: Heat flow measured for the slag blends at (a) 20℃ and (b) 38℃, Total heat evolved by the slag blends at (c) 20℃ and (d) 38℃ . Mix 'PC' contains 100% of CEM I 52.5R, while mix 'PC-30Q' contains 70% CEM I 52.5R and 30% Quartz.

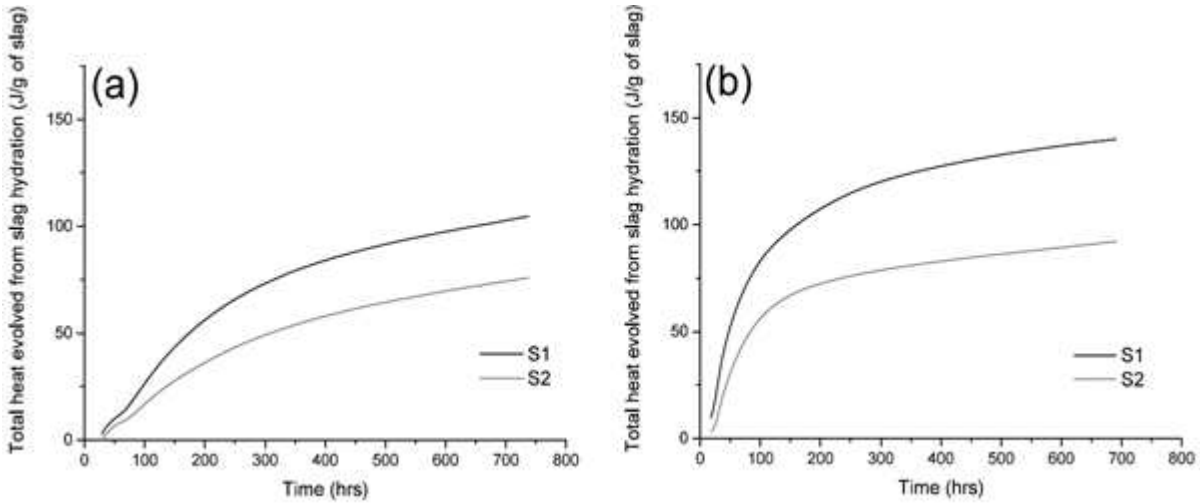

Fig. 5: Slag contribution to total heat evolved at (a) 20℃ (b) 38℃

3.2.2 Impact of temperature on the heat of hydration:

High temperature curing resulted in greater early-stage heat evolution. This is observed in **Error! Reference source not found.**c and **Error! Reference source not found.**d, where at 38℃ the total heat curves appeared to be steeper at ea rly ages up to about 50 hrs, after which there was minimal increase. Conversely, at 20℃ initial heat evolution was lower, but continued for longer. At the end of the measurement period (at about 720 hrs), the total heat evolved at 20 and 38℃ was similar for each mix, indicating that the overall extent of reaction was the same. For the heat flow curves (**Error! Reference source not found.**a and **Error! Reference source not found.**b), peaks II and III corresponding to the formation of C-S-H and renewed ettringite [19, 45] are observed after about 15 hours from the start of the reaction at 20℃ compared to after about 7 hours at 38℃. Peaks II and III we re almost coincident at 20℃; whereas at 38℃, while both peaks appeared sooner, they also sharpened, such that there was a clear distinction between both peaks. The reason for this is because at higher temperatures, there is an increased quantity of C-S-H due to the increased rate of hydration. Also, with increasing temperature there is an increase in the amount of sulphate ions reversibly bound to the C-S-H phase, such that fewer sulphates are available to react and form AFt [46-48]. This was clearly reflected in **Error! Reference source not found.**b, where the intensity of peak III was much lower than that of peak II; whereas in **Error! Reference source not found.**a, both peaks had similar intensities. The formation of the AFm phases, which is represented by peak IV [45], was visible at 20℃, but not at 38℃. This indicates that at the hig her temperature, the AFt to AFm conversion occurred very early on such that peak IV was hidden underneath peaks II and III. This can be attributed to the accelerating effect of

280 temperature on the early stages of hydration [46, 49], and explains the reason for the
281 initial higher strengths observed at 38℃ in Fig. 3.
282 From Table 5, it can be seen that the maximum peak heat flow (q_{max}) measured for
283 the slag blends at 38℃ was about three-times that measured at 20° C, and the time
284 taken to reach q_{max} at 38℃ was about one-third of that at 20℃. Previous studies [18-
285 21] have reported that at higher temperatures, GGBS contributes more to the total
286 heat of hydration than at lower temperatures. Indeed, from **Error! Reference source**
287 **not found.**a and **Error! Reference source not found.**b, it can be seen that the
288 contribution to the total heat from the hydration of the slags was far greater at 38℃
289 than at 20℃. This explains the shorter times taken to reach q_{max} at 38℃, and indicates
290 that at 38℃ the slags reacted more rapidly and contributed to the heat released in the
291 system. However, despite the increased slag hydration at 38℃, this was not clearly
292 reflected on the overall total heat evolved by the slag blends at 38°C, as seen at the
293 later stages (at about 720 hrs) in **Error! Reference source not found.**c and **Error!**
294 **Reference source not found.**d. This is because the total heat evolved by the neat
295 CEM I at about 720 hrs, is greater at 20℃ than at 38℃, thus masking the increased
296 contribution from the slag hydration at the higher temperature. This would explain why
297 towards the later stages of the measurement, the total heat evolved from each slag
298 blend was almost independent of temperatures. This indicates that high temperature
299 favours the reactivity of slags more than that of clinker and is in agreement with
300 previous findings [22, 27, 50]. Although it can be seen that the higher temperature
301 accelerated the hydration of slag 1 more than slag 2.

Table 5: Maximum peak heat flow (q_{max}) and time taken to reach q_{max}

	20℃		38℃	
	q_{max} (mW/g of PC)	Time (hrs)	q_{max} (mW/g of PC)	Time (hrs)
S1	5.24	13.70	19.85	4.55
S2	4.98	14.95	18.29	4.81

3.2.3 Impact of slag composition on heat of hydration:

Both heat flow and total heat evolution was greater for S1 (the more-basic, high alumina slag blend) than for S2 at both temperatures, and is in agreement with previous findings [51, 52]. Furthermore, the total heat evolved by S1 compared to S2, was far more at 38℃ than it was at 20℃. This can be seen clearl y by comparing **Error! Reference source not found.**a and **Error! Reference source not found.**b. At both temperatures, the q_{max} of S1 was higher than that of S2. Since the level of replacement was the same for both mixes, the higher values of q_{max} obtained for S1 indicates that slag 1 had a higher degree and rate of hydration. This correlates with the compressive strength results shown in Fig. 3. The reason for this can be attributed to the lower activation energy of the slag 1 blend (discussed in the next section), which is a consequence of its chemical composition. Richardson et al. [19] observed for slag blends that the reaction of the silicates and aluminates were accelerated at higher temperatures. Since slag 1 has a higher alumina content than slag 2 (as seen in Table 1), the higher temperature would accelerate its reaction more than that of slag 2.

3.2.4 Activation energy of the slags

The activation energy of the slag blends was determined from the cumulative heat flow, by applying an Arrhenius-type equation as shown below [5, 20]:

$$\frac{t_1}{t_2} = exp\frac{E}{R}\left(\frac{1}{T_1} - \frac{1}{T_2}\right) \quad (5)$$

Where t_1 and t_2 = time at 50% degree of hydration at temperatures T_1 and T_2 (in Kelvin) respectively, E = activation energy in kJ/mol, and R = gas constant taken as 8.314 $JK^{-1}mol^{-1}$.

Activation energies of 43.65 and 44.57 kJ/mol were obtained for slag 1 and 2 blend respectively, within the range reported for slag blends [5, 20, 24]. The activation energy of the slag 1 blend is slightly lower than that of the slag 2 blend, explaining why the accelerating effect of temperature was more pronounced on the slag 1 blend than the slag 2 blend.

3.2.5 XRD analysis

XRD analysis was carried out to examine the influence of temperature on hydration and phase assemblage. **Fig. 6** shows a section of the XRD patterns obtained from both slag blends after hydration at 20 and 38^{o}C for 1, 7 and 28 days. As observed by calorimetry, the high temperature accelerated the early hydration of the clinker phases. After 1 day there was no trace of C_3A in the samples cured at 38℃ and the peaks of C_3S and C_2S were much less intense than those from the samples cured at 20℃. At later ages of 7 and 28 days, the C_3S and C_2S peaks were of similar intensities at both temperatures. Also **Fig. 6** indicated that, at both temperatures, the blends containing slag 1 contained less portlandite than those containing slag 2, thus implying that slag 1 had reacted more than slag 2. This is in line with the results of the isothermal calorimetry shown in **Error! Reference source not found.**, and will be discussed further in 3.2.7.

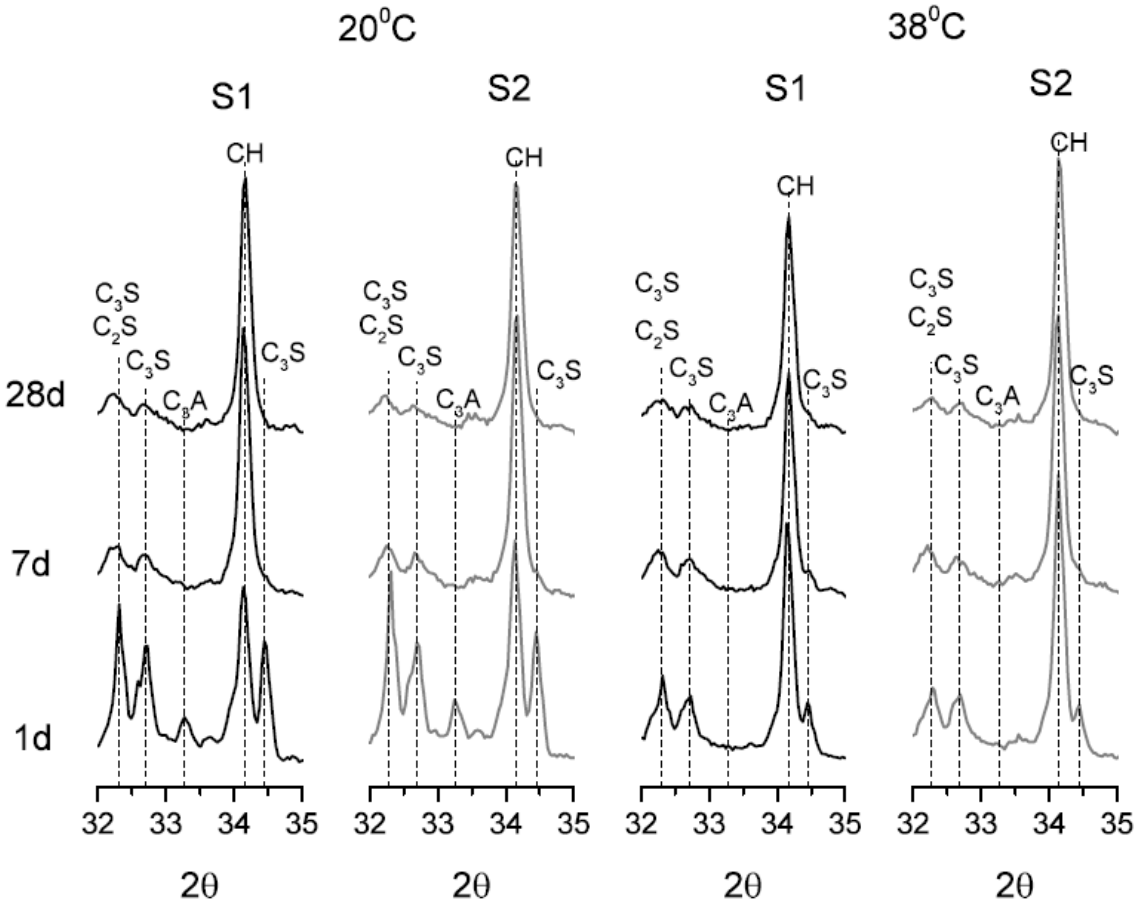

Fig. 6: XRD patterns of paste samples showing the effect of temperature on the initial hydration of the slag blends

Fig. 7 shows the impact of temperature on the evolution of the AFt and AFm phases for all the mixes at 20 and 38℃. Ettringite (E), which is the main AFt p hase had less intense reflections at the higher temperature for all the samples, as was observed by Lothenbach et al. [50]. This is because higher temperatures accelerate the conversion of AFt to AFm [46-48].

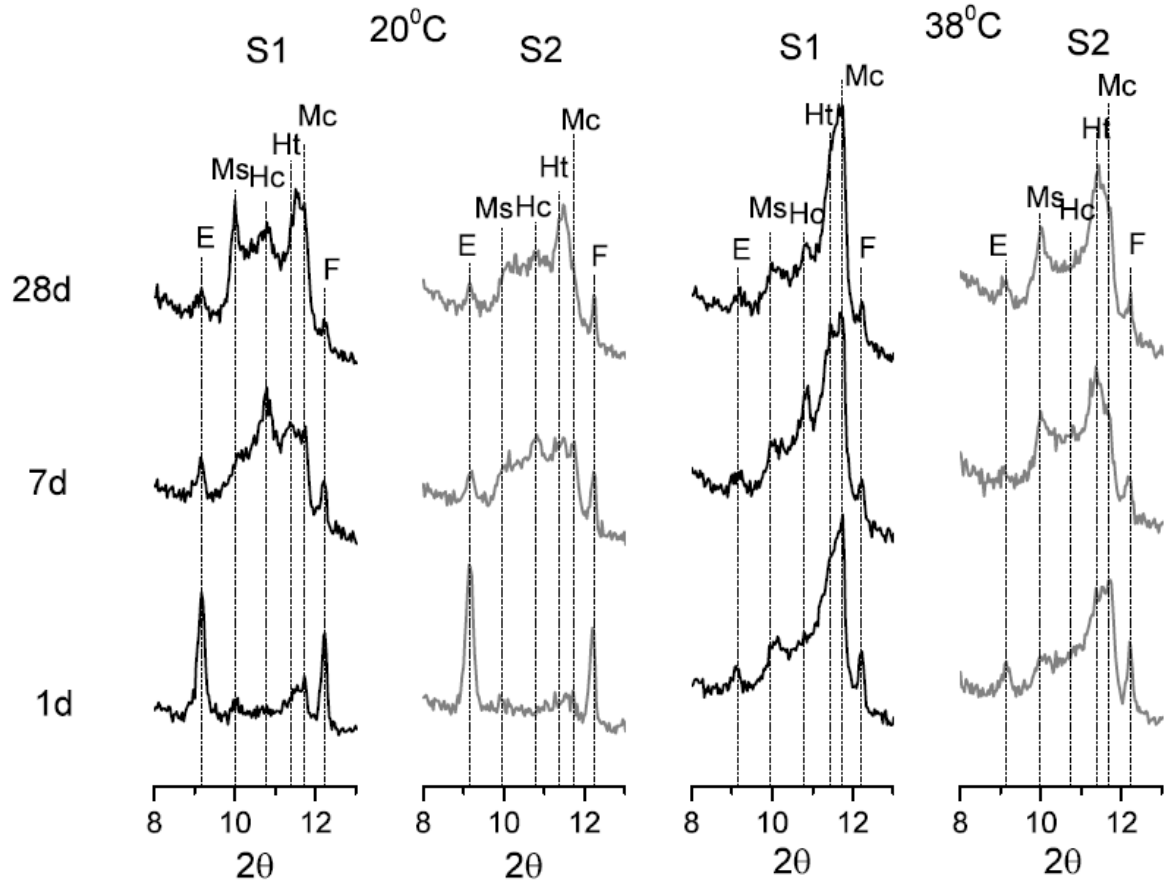

E – Ettringite, Ms – Calcium monosulfoaluminate, Hc – Calcium hemicarboaluminate, Ht – Hydrotalcite, Mc – Calcium monocarboaluminate, F - Ferrite

Fig. 7: XRD patterns of paste samples showing the effect of temperature on the evolution of the Aft and AFm phases

The accelerating effect of temperature on the early hydration of C_3A can also be seen from Fig. 7, where, after 1 day, the reflections due to the AFm phases (monosulfoaluminate – Ms, hemicarboaluminate – Hc, monocarboaluminate – Mc) are more prominent at 38℃ than at 20℃, and supports the earlier obse rvation in the heat flow measurements (shown in **Error! Reference source not found.**). This indicates that the reaction of C_3A occurred at a faster rate at the higher temperature. This may be due to the unavailability of sulphate ions at the higher temperature, due to increased uptake by C-S-H, inducing the reaction of C_3A with water (a reaction which

is known to occur at a much faster rate). Indeed, XRD patterns of 1 day old paste samples clearly showed weak reflections for gypsum at 2θ angle of about 23.4° (as shown in Fig. 8). This explains why peak IV was not clearly visible at the higher temperature, as seen in the heat flow curve shown in **Error! Reference source not found.**b.

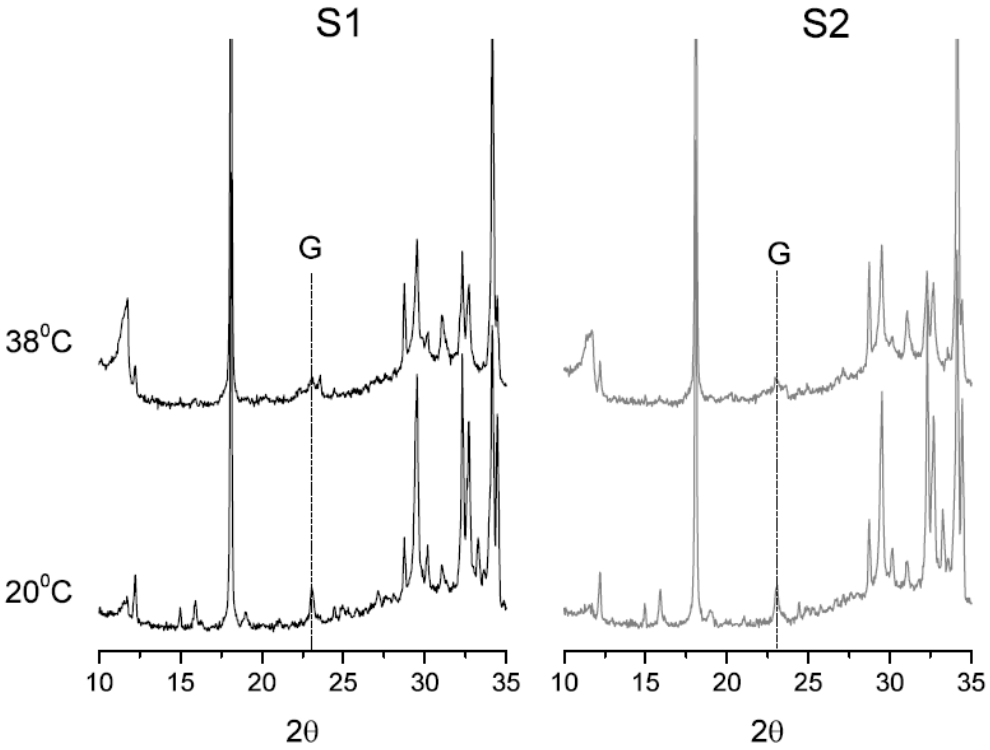

Fig. 8: XRD patterns of 1 day old paste samples showing the depletion of gypsum (G) for samples cured at 38℃

The reflection for hydrotalcite (Ht), a product of slag hydration [53-55], overlapped with that of Mc, and was more prominent after 1 day at the higher temperature, indicating that the early hydration of the slags was accelerated at the higher temperature. This correlates with the calorimetry results (**Error! Reference source not found.**). The reflections for Hc were more prominent in the aluminium-rich slag blend (S1) as observed by Whitaker et al. [32], and temperature did not seem to have any impact on the amount formed except at 1 day. At 38℃, Mc was formed at the expense of Ms for

377 the slag 1 blend. For the slag 2 blend, the amount of Hc decreased progressively and
378 was barely noticeable after 28 days especially at the higher temperature, due to the
379 conversion of Hc to Mc. The reflections for Ms and Ht were more prominent at 38℃
380 than at 20℃ for the slag 2 blend. The higher temperature did not have a ny significant
381 effect on the amount of Mc formed for the slag 2 blend, as compared to the slag 1
382 blend.
383 Overall, in terms of the hydration products formed in both slag blends, the reflections
384 due to Ms were slightly less intense for S1 than for S2, but the reflections due to Ht
385 and Mc were more prominent for S1 than for S2 at both temperatures, but especially
386 at the higher temperature. This reflects the higher degree of hydration of slag 1 than
387 slag 2 at 38℃, and possibly also the higher aluminium content of slag 1. It also
388 correlates with the calorimetry and compressive strength results shown in **Error!**
389 **Reference source not found.** and Fig. 3 respectively.
390 3.2.6 BSE-SEM image analysis
391 Table 6 shows the degree of slag hydration, as determined by BSE-SEM image
392 analysis, of 7 and 28 day old paste samples cured at 20 and 38°C. The results followed
393 the same trend as the calorimetry and XRD (**Error! Reference source not found.**
394 and **Fig. 6**), where it was seen that the higher temperature increased the rate of slag
395 hydration. The higher temperature resulted in an increase in the degree of slag
396 hydration, especially at early age. At 7 days, the degree of hydration of slag 1 and slag
397 2 at 38℃ was greater than that of 20℃ by about 14 and 11 percen tage points
398 respectively. By 28 days, this difference had fallen to about 8 and 5 percentage points
399 for slag 1 and slag 2 respectively.
400 In terms of the impact of the chemical composition of the slags, the more reactive slag
401 1 had hydrated to a greater extent than slag 2, at both ages and curing temperatures.

At 20℃, the degree of hydration of slag 1 was about 8 and 11 percent age points higher than that of slag 2 at 7 and 28 days respectively; while at 38℃, this became about 11 and 13 percentage points at 7 and 28 days respectively. At 38℃, as the curing duration was increased from 7 to 28 days, the degree of hydration of slag 1 was increased by about 9 percentage points compared to about 6 percentage points for slag 2. This indicates that slag 1 responded more to the higher temperature, as was previously observed by calorimetry and XRD.

Table 6: Degree of hydration (%) of the slag blends at 7 and 28 days

Mix	Temperature	7 day	Error	28 day	Error
S1	20℃	39.64	1.29	54.85	1.00
	38℃	53.29	1.12	62.40	1.01
S2	20℃	31.81	1.84	43.76	1.55
	38℃	42.44	1.76	48.92	1.50

3.2.7 Portlandite and bound water content

Thermal gravimetric analysis was performed to follow the development of portlandite and bound water contents over a period of 6 months. These are shown in Fig. 9 and Fig. 10 respectively.

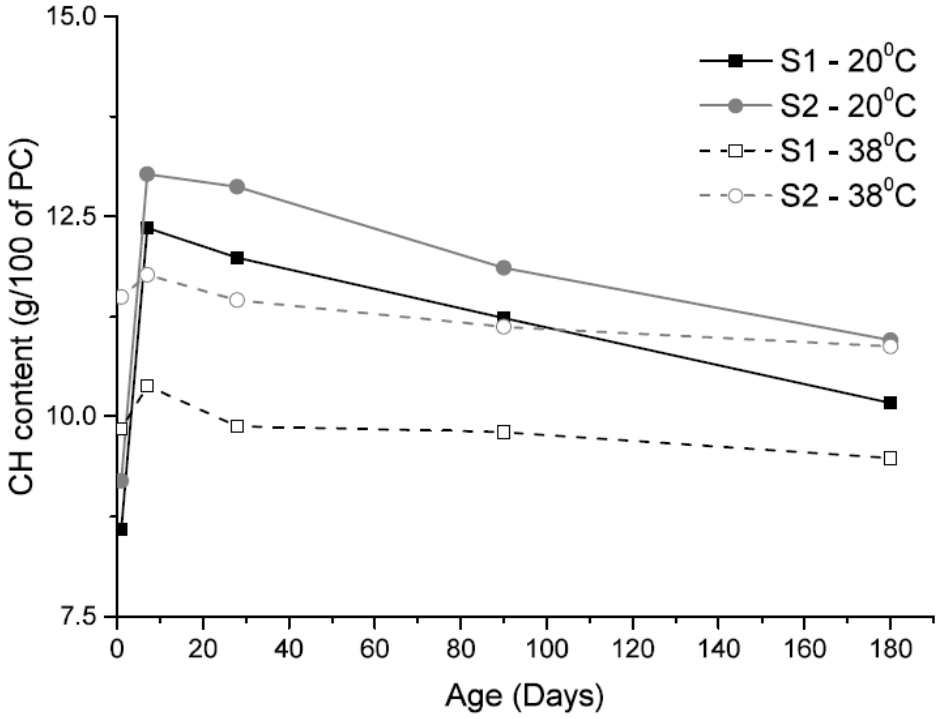

Fig. 9: Portlandite content from STA for all mixes at 20 and 38℃

For both blends, the portlandite content measured after 1 day at 38℃ was significantly higher than that measured at 20℃. This reflects the accelerated initial hydration o f the clinker at high temperature, as also observed by calorimetry and XRD. The portlandite content of the blends rose initially then decreased steadily over time due to its consumption during slag hydration [17, 26, 56]. This supports previous observations that slag hydration is gradual and continues for long periods [32, 33, 57]. After 7 days and beyond, the portlandite contents were lower following curing at higher temperatures than at lower temperatures, reflecting the greater degree of slag hydration. S1 had lower portlandite contents than S2 at both temperatures, with the difference being much higher at 38℃ . This reflects the increased reactivity of slag 1 over slag 2 at the higher temperature as observed previously by calorimetry, XRD and SEM, and explains the significant difference observed in the strength development of these two blends at 38℃ (as seen in Fig. 3).

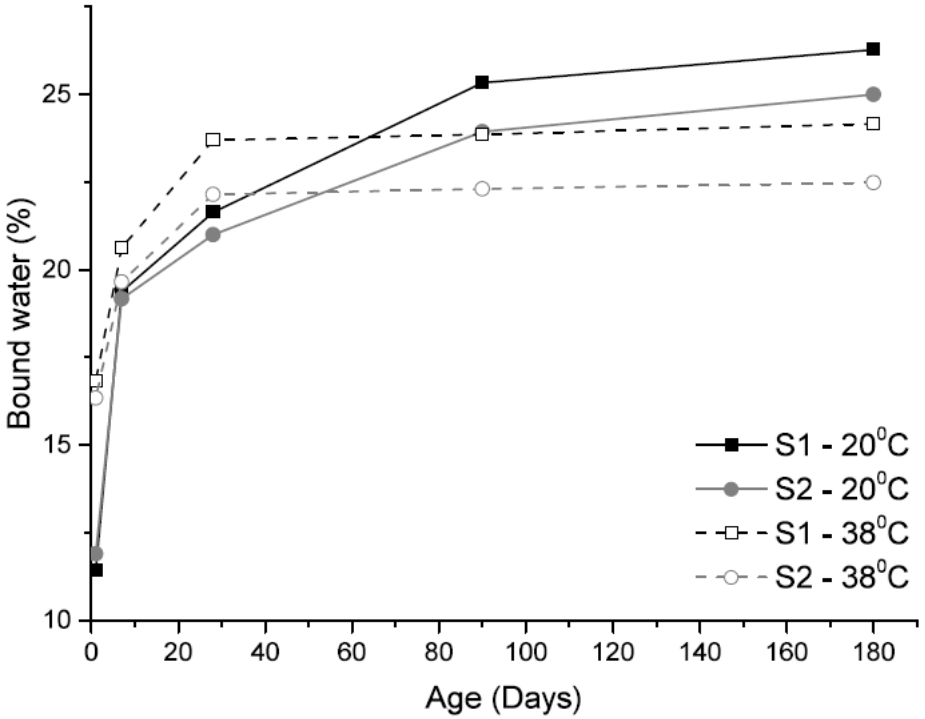

Fig. 10: Bound water content from STA for all mixes at 20 and 38℃

There was a steady increase in bound water content with time (Fig. 10), indicating an increase in the overall degree of hydration. The bound water content was initially higher for the samples cured at 38℃ than those cured at 20℃, but was lower at later ages. Furthermore, the bound water content of the samples cured at the higher temperature did not increase much beyond 28 days. This can be attributed to the impact of high temperature curing. High temperature curing results in a high initial rate of hydration, retarding subsequent hydration [24, 40, 50]. It should be noted that the bound water content at 38℃ was not corrected for any changes in th e water content of the hydrates as a function of temperature. Gallucci et al. [58] observed that the bound water content of C-S-H was reduced by about 14.5% when the temperature was increased from 5 to 60℃. If we take this into consideration at 38℃, and ignore minor contributions to the bound water content due to CH and AFt, the degree of hydration at the later ages would be similar at both temperatures, as was observed when comparing the portlandite contents. The bound water content of S1 was higher

than that of S2 at both temperatures, indicating the increased reactivity of slag 1. Also, it was observed that the difference between the bound water content of S1 and S2 blend was greater at 38℃ than at 20℃, as was seen in the compressive strength, calorimetry, and SEM results.

3.3 Pore structure

3.3.1 Determination of coarse capillary porosity

Fig. 11 and Fig. 12 shows selected BSE-SEM images obtained from samples cured for 7 and 28 days. The samples cured at 38℃ for 7 days had a lower apparent porosity than the ones cured at 20℃. The reason for this can be attributed to the increased reactivity of the slags at 38℃ as discussed previously. Anguski da Luz and Hooton [51] observed that paste samples made from super sulphated cements and cured for 7 days at higher temperatures had similarly lower porosities than ones cured at lower temperatures. After 7 days (as shown in Table 6), the degree of slag hydration in the samples cured at 38℃ was about 53% for slag 1 and 42% for slag 2, compared to about 40% and 32% at 20℃. These additional hydration products at early stages will have a pore blocking effect on the microstructure [8]. This reduced porosity at 7 days observed for the slag blends at 38℃ was reflected in the strength results (Fig. 3), where the slag blends had greater early age strengths at 38℃ than at 20 ℃. However, on prolonged curing for 28 days, samples cured at 38℃ had greater apparent porosities than those cured at 20℃. The reason for this can also be linked to the reactivity of the slags at 38℃. From Table 6, after 28 days there was only slight difference in the degree of hydration of the slags at 20 and 38℃. This, coupled with the effect of prolonged high temperature curing on the microstructure, would explain why the porosity of the samples cured for 28 days at 38℃ became greater than those

cured at 20℃. This indicates that prolonged curing at the lower temperature was m ore beneficial for the microstructural development of the slag blends.

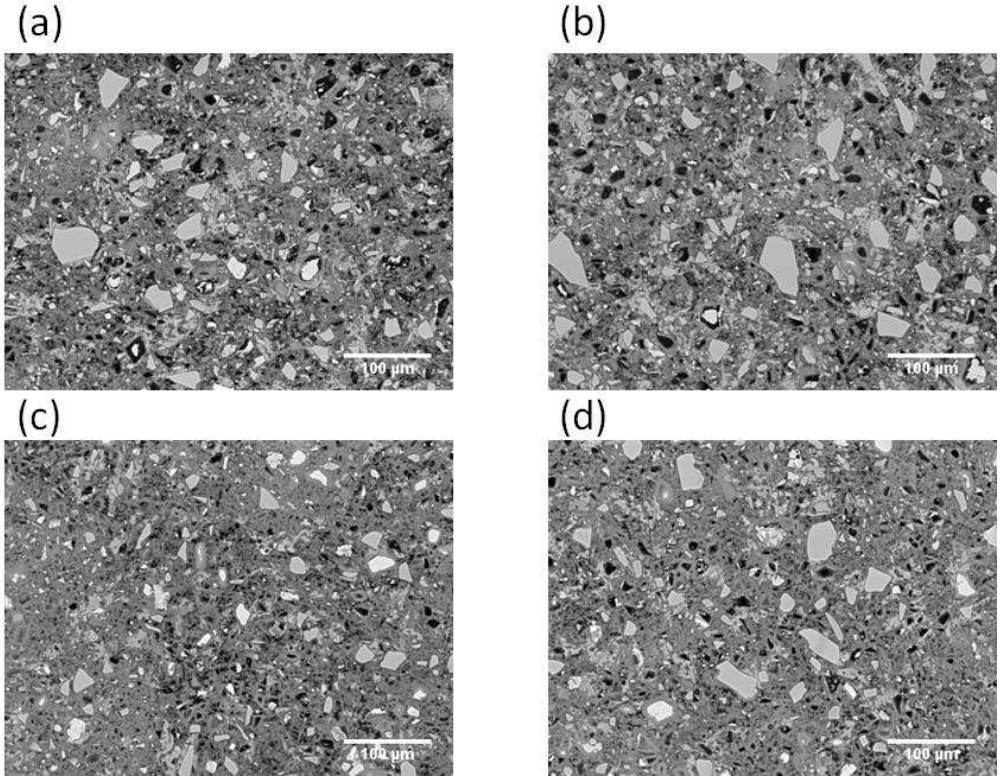

Fig. 11: BSE-SEM images of 7 day old paste samples (a) S1 at 20℃ (b) S2 at 20℃ (c) S1 at 38℃ (d) S2 at 38℃

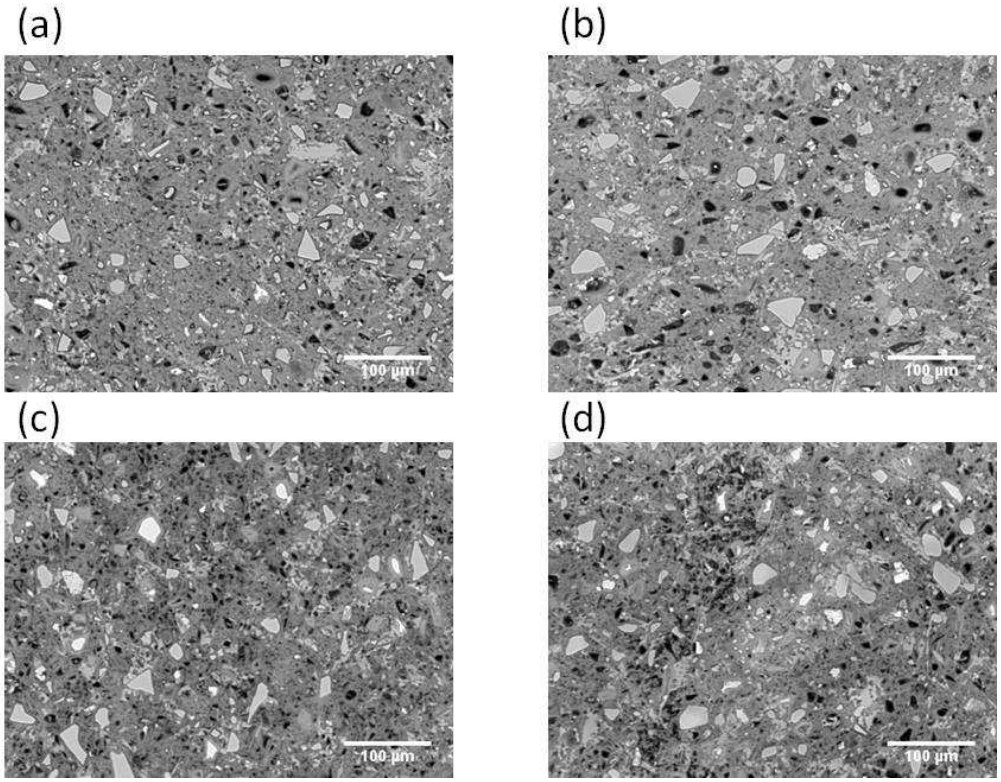

475

476 **Fig. 12:** BSE-SEM images of 28 day old paste samples (a) S1 at 20℃ (b) S2 at
477 20℃ (c) S1 at 38℃ (d) S2 at 38℃

478 The coarse porosities, as determined from the electron images, are shown in Table 7.
479 At 7 days, the coarse porosity of the samples cured at 38℃ was about 25% low er than
480 that of the 20℃ samples but at 28 days this reversed and the coarse porosity became
481 about 35% higher.

482 Comparing the 2 slags, the blends prepared with slag 1 always showed a lower coarse
483 porosity than the equivalent blend prepared with slag 2. Furthermore, the difference in
484 performance between the 2 slags increased with increasing temperature. This
485 correlates with the previous results and further explains why samples prepared with
486 slag 1 had higher strengths than those prepared with slag 2.

Table 7: Degree of porosity (%) of the slag blends at 7 and 28 days

Mix	Temperature	7 days	Error	28 days	Error
S1	20℃	11.75	0.10	6.54	0.11
	38℃	9.21	0.14	8.87	0.08
S2	20℃	12.27	0.12	7.03	0.07
	38℃	9.88	0.11	9.48	0.09

3.3.2 Sorptivity

Table 8 shows the sorptivity of 28 and 90 day old samples which had been cured at 20 and 38℃. As was observed with coarse porosity, the sorptivities of blends prepared with slag 1 were lower than those for slag 2 blends at both temperatures. This is due to the greater degree of hydration and subsequent finer pore structure in the more reactive slag blends [59]. The 90 day sorptivity was lower than the 28 day sorptivity for both slag blends at both temperatures, thus indicating that the slags continued to hydrate thereby resulting in the formation of a denser microstructure. At 20℃, the 28 day sorptivity of S2 was about 60% higher than that of S1, but at 90 days this reduced to about 35%. This highlights the impact of prolonged curing on the microstructural development of the slag 2 blend and would explain why both slag blends had similar later-age strengths at 20℃ as seen in Fig. 3 .

Curing at elevated temperature resulted in a significant increase in sorptivity. At 28 days, the sorptivity of both slag blends was about 90% higher in the samples cured at 38℃ compared to those cured at 20℃. After 90 days this difference increased to about 160% and 200% for S1 and S2 respectively, indicating that the high temperature curing was more detrimental to the microstructure of the less-reactive slag 2. This supports the compressive strength results and explains the lower later-age strengths

observed for the samples cured at 38℃, and the larger difference observed between the compressive strengths of the slag blends cured at 38℃.

Table 8: Effect of curing age and temperature on sorptivity

Mix	Age	Sorptivity, k ($m^3/m^2s^{1/2}$)x10^{-5}	
		20℃	38℃
S1	28 days	2.08 ± 0.05	3.96 ± 0.07
	90 days	1.37 ± 0.04	3.55 ± 0.08
S2	28 days	3.32 ± 0.09	6.36 ± 0.04
	90 days	1.85 ± 0.07	5.60 ± 0.04

4. Summary and conclusions

This study has examined the performance and microstructure of 30% replacement slag cement blends, and looked at the combined influence of temperature and a difference in slag chemical composition. High temperature curing was seen to increase the early strength of all the mixes, but not the later strength. Beyond 28 days, there was minimal strength increase at 38℃ while the samples cured at 20℃ continued to gain strength. This was attributed to the effect of high temperature curing on hydration, which would accelerate the early hydration, and slow down subsequent hydration.

In terms of the strength performance of the slag blends, at 20℃ both slag blends showed similar strength development, especially at later ages. Conversely, at 38℃ there was a clear difference in performance, with slag 1, the more basic of the 2 slags, performing better than slag 2 at all ages. Although, the higher temperature increased the reactivity of the slags, the effect was seen to be greater on slag 1 (the more reactive slag). This was attributed to the chemical composition of slag 1 leading to a

lower activation energy. The strength performance of the blends tallied with the predictions of the slag activity index and basicity index at 20℃ and 38℃ respectiv ely. Increased degrees of hydration are known to reduce porosity. However, the results have shown that the degree of hydration alone cannot explain porosity and transport properties. Rather, temperature has been shown to have a great impact. For all the samples studied, high temperature curing was seen to increase the degree of capillary porosity and rate of water penetration. The effect of the high temperature curing was more pronounced on the slag 2 blend. Regardless of the temperature and curing duration, the slag 1 blend had lower porosities and exhibited better transport properties than the slag 2 blend. This was attributed to the higher reactivity of slag 1. Prolonged curing at 20℃ led to significant improvements in the microstructure and transp ort properties of the slag blends. However, this impact was seen to be greater for the slag 2 blend.

Although, it has been shown in previous studies that the reactivity of slag is greatly influenced by the chemical composition of the slag, this study has further shown that this influence is dependent on the hydration temperature. At the lower temperature of 20℃, difference in chemical composition of the slags did not seem to hav e any significant impact on the strength and transport properties of the slag blends studied, especially at the later ages; whereas it did at all ages, at the higher temperature of 38℃. This indicates that in hot climates, like the tropical regions, to achiev e good performance, slag blends should be prepared from slags of higher basicity or higher alumina contents. While both slags used in the study met with the requirements as specified in BS EN 197-1:2011 [9] and BS EN 15167 [3], and performed well at the lower temperature, the results clearly showed that the compositional requirements are more exacting at higher temperatures.

Acknowledgement

The authors would like to thank the Petroleum Technology Development Fund (PTDF) of Nigeria for providing the funds for this research and Dr Maciej Zajac of Heidelberg Technology Centre GmbH for his comments and contributions.

REFERENCES

[1] Hadj-sadok A, Kenai S, Courard L, Darimont A. Microstructure and durability of mortars modified with medium active blast furnace slag. Construction and Building Materials. 2011;25(2):1018-25.

[2] Shi X, Xie N, Fortune K, Gong J. Durability of steel reinforced concrete in chloride environments: An overview. Construction and Building Materials. 2012;30:125-38.

[3] EN15167-1:2006. Definitions, specifications and conformity criteria. Ground granulated blast furnace slag for use in concrete, mortar and grout. Brussels: BSI.

[4] ASTMC989/C989M-14. Standard Specification for Slag Cement for Use in Concrete and Mortars. West Conshohocken, PA: ASTM International; 2014.

[5] Moranville-Regourd M. Cements Made from Blastfurnace Slag. Lea's Chemistry of Cement and Concrete2003. p. 637-78.

[6] ACI-233R-03. Slag Cement in Concrete and Mortar Farmington Hills, MI: American Concrete Institute; 2003. p. 18.

[7] Swamy RN. Design for durability and strength through the use of fly ash and slag in concrete. CANMET/ACI International Workshop on Supplementary Cementing Materials, Superplasticizers and Other Chemical Admixtures in Concrete. Toronto, Canada: American Concrete Institute; 1998. p. 1-72.

[8] Siddique R, Bennacer R. Use of iron and steel industry by-product (GGBS) in cement paste and mortar. Resources, Conservation and Recycling. 2012;69(0):29-34.

[9] EN197-1:2011. Composition, specifications and conformity criteria for common cements. Brussels: BSI. p. 1.

[10] Pal SC, Mukherjee A, Pathak SR. Investigation of hydraulic activity of ground granulated blast furnace slag in concrete. Cement and Concrete Research. 2003;33(9):1481-6.

[11] Haha MB, Lothenbach B, Le Saout G, Winnefeld F. Influence of slag chemistry on the hydration of alkali-activated blast-furnace slag — Part II: Effect of Al2O3. Cement and Concrete Research. 2012;42(1):74-83.

[12] Satarin V. Slag portland cement. The proceedings of the sixth internatinal congress of Chem Cem(VI ICCC), Moscow1974. p. 1-51.

[13] Wang PZ, Trettin R, Rudert V, Spaniol T. Influence of Al2O3 content on hydraulic reactivity of granulated blast-furnace slag, and the interaction between Al2O3 and CaO. Advances in Cement Research. 2004;16(1):1-7.

[14] Haha MB, Lothenbach B, Saout GL, Winnefeld F. Influence of slag chemistry on the hydration of alkali-activated blast-furnace slag - Part I: Effect of MgO. Cement and Concrete Research. 2011;41(9):955-63.

[15] Smolczyk MG. Effect of the chemistry of the slag on the strengths of blast furnace slags. Zement-kalk-Gips. Wiesbaden1979. p. 294-6.

[16] Mantel DG. Investigation into the hydraulic activity of five granulated blast furnace slags with eight different portland cements. ACI Materials Journal. 1994;91(5):471-7.

[17] Bougara A, Lynsdale C, Milestone NB. Reactivity and performance of blastfurnace slags of differing origin. Cement and Concrete Composites. 2010;32(4):319-24.

[18] Escalante-Garcia JI, Sharp JH. The effect of temperature on the early hydration of Portland cement and blended cements. Advances in Cement Research. 2000;12(3):121-30.

[19] Richardson IG, Wilding CR, Dickson MJ. The hydration of blastfurnace slag cements. Advances in Cement Research. 1989;2(8):147-57.

[20] Wu X, Roy DM, Langton CA. Early stage hydration of slag-cement. Cement and Concrete Research. 1983;13(2):277-86.

[21] Ma W, Sample D, Martin R, Brown PW. Calorimetric study of cement blends containing fly ash, silica fume, and slag at elevated temperatures. Cement, Concrete and Aggregates. 1994;16(2):93-9.

[22] Escalante-García JI, Sharp JH. Effect of temperature on the hydration of the main clinker phases in portland cements: part ii, blended cements. Cement and Concrete Research. 1998;28(9):1259-74.

[23] Escalante JI, Gómez LY, Johal KK, Mendoza G, Mancha H, Méndez J. Reactivity of blast-furnace slag in Portland cement blends hydrated under different conditions. Cement and Concrete Research. 2001;31(10):1403-9.

[24] Barnett SJ, Soutsos MN, Millard SG, Bungey JH. Strength development of mortars containing ground granulated blast-furnace slag: Effect of curing temperature and determination of apparent activation energies. Cement and Concrete Research. 2006;36(3):434-40.

[25] Çakır Ö, Aköz F. Effect of curing conditions on the mortars with and without GGBFS. Construction and Building Materials. 2008;22(3):308-14.

[26] Kolani B, Buffo-Lacarrière L, Sellier A, Escadeillas G, Boutillon L, Linger L. Hydration of slag-blended cements. Cement and Concrete Composites. 2012;34(9):1009-18.

[27] Wang Q, Miao M, Feng J, Yan P. The influence of high-temperature curing on the hydration characteristics of a cement - GGBS binder. Advances in Cement Research2012. p. 33-40.

[28] Hewlett PC. Lea's chemistry of cement and concrete. 4th ed. Oxford: Elsevier Butterworth-Heinmann; 2004.

[29] EN196-1:2005. Methods of testing cement. Determination of strength. Brussels: BSI.

[30] Kocaba V. Development and evaluation of methods to follow microstructural development of cementitious systems including slags [PhD Thesis]. Lausanne, Switzerland: Ecole Polytechnique Federale De Lausanne; 2009.

[31] Lothenbach B, Scrivener K, Hooton RD. Supplementary cementitious materials. Cement and Concrete Research. 2011;41(12):1244-56.

[32] Whittaker M, Zajac M, Ben Haha M, Bullerjahn F, Black L. The role of the alumina content of slag, plus the presence of additional sulfate on the hydration and microstructure of Portland cement-slag blends. Cement and Concrete Research. 2014;66(0):91-101.

[33] Kocaba V, Gallucci E, Scrivener KL. Methods for determination of degree of reaction of slag in blended cement pastes. Cement and Concrete Research. 2012;42(3):511-25.

[34] Feng X, Garboczi EJ, Bentz DP, Stutzman PE, Mason TO. Estimation of the degree of hydration of blended cement pastes by a scanning electron microscope point-counting procedure. Cement and Concrete Research. 2004;34(10):1787-93.

[35] Scrivener KL. Backscattered electron imaging of cementitious microstructures: understanding and quantification. Cement and Concrete Composites. 2004;26(8):935-45.

[36] Lange DA, Jennings HM, Shah SP. Image analysis techniques for characterization of pore structure of cement-based materials. Cement and Concrete Research. 1994;24(5):841-53.

[37] Wong HS, Head MK, Buenfeld NR. Pore segmentation of cement-based materials from backscattered electron images. Cement and Concrete Research. 2006;36(6):1083-90.

[38] Tasdemir C. Combined effects of mineral admixtures and curing conditions on the sorptivity coefficient of concrete. Cement and Concrete Research. 2003;33(10):1637-42.

[39] Güneyesi E, Gesoğlu M. A study on durability properties of high-performance concretes incorporating high replacement levels of slag. Mater Struct. 2008;41(3):15.

[40] Brooks JJ, Al-kaisi AF. Early strength development of Portland and slag cement concretes cured at elevated temperatures. ACI Materials Journal. 1990;87:503-7.

[41] Stutterheim H. Properties and uses of high-magnesia portland slag cement concretes. Journal of the American Concrete Society. 1960:1027-45.

[42] Otieno M, Beushausen H, Alexander M. Effect of chemical composition of slag on chloride penetration resistance of concrete. Cement and Concrete Composites. 2014;46(0):56-64.

[43] Gutteridge WA, Dalziel JA. Filler cement: The effect of the secondary component on the hydration of Portland cement: Part 2: Fine hydraulic binders. Cement and Concrete Research. 1990;20(6):853-61.

[44] Berodier E, Scrivener K. Understanding the Filler Effect on the Nucleation and Growth of C-S-H. Journal of the American Ceramic Society. 2014;97(12):3764-73.

[45] Taylor HFW. Cement chemistry. 2nd ed. London: Thomas Telford Publishing; 1997.

[46] Kjellsen KO, Detwiler RJ. Reaction kinetics of portland cement mortars hydrated at different temperatures. Cement and Concrete Research. 1992;22(1):112-20.

[47] Odler I, Abdul-Maula S, Zhongya L. Effect of hydration temperature on cement paste structure. MRS Proceedings: Cambridge Univ Press; 1986. p. 139.

[48] Sylla H. Reactions in cement stone due to heat treatment. Benton. 1988;38(11):449-54.

[49] Odler I. Hydration, Setting and Hardening of Portland Cement. Lea's Chemistry of Cement and Concrete2003. p. 241-97.

[50] Lothenbach B, Winnefeld F, Alder C, Wieland E, Lunk P. Effect of temperature on the pore solution, microstructure and hydration products of Portland cement pastes. Cement and Concrete Research. 2007;37(4):483-91.

[51] Angulski da Luz C, R. D H. Influence of curing temperature on the process of hydration of supersulfated cements at early age. Cement and Concrete Research. 2015;77:69-75.

[52] Gruskovnjak A, Lothenbach B, Winnefeld F, Figi R, Ko SC, Adler M, et al. Hydration mechanisms of super sulphated slag cement. Cement and Concrete Research. 2008;38(7):983-92.

[53] Ben Haha M, Le Saout G, Winnefeld F, Lothenbach B. Influence of activator type on hydration kinetics, hydrate assemblage and microstructural development of alkali activated blast-furnace slags. Cement and Concrete Research. 2011;41(3):301-10.

[54] Lumley JS, Gollop RS, Moir GK, Taylor HFW. Degrees of reaction of the slag in some blends with Portland cements. Cement and Concrete Research. 1996;26(1):139-51.

[55] Richardson JM, Biernacki JJ, Stutzman PE, Bentz DP. Stoichiometry of Slag Hydration with Calcium Hydroxide. Journal of the American Ceramic Society. 2002;85(4):947-53.

[56] Pane I, Hansen W. Investigation of blended cement hydration by isothermal calorimetry and thermal analysis. Cement and Concrete Research. 2005;35(6):1155-64.

[57] Taylor R, Richardson IG, Brydson RMD. Composition and microstructure of 20-year-old ordinary Portland cement–ground granulated blast-furnace slag blends containing 0 to 100% slag. Cement and Concrete Research. 2010;40(7):971-83.

[58] Gallucci E, Zhang X, Scrivener KL. Effect of temperature on the microstructure of calcium silicate hydrate (C-S-H). Cement and Concrete Research. 2013;53(0):185-95.

[59] Chen HJ, Huang SS, Tang CW, Malek MA, Ean LW. Effect of curing environments on strength, porosity and chloride ingress resistance of blast furnace slag cement

717 concretes: A construction site study. Construction and Building Materials.
718 2012;35:1063-70.